Laboratory Investigation (2020) 100:643–656
https://doi.org/10.1038/s41374-019-0332-8

ARTICLE

Polydatin protects against lipopolysaccharide-induced endothelial barrier disruption via SIRT3 activation

Jie Wu[1,2] · Zhiya Deng[1,2] · Maomao Sun[1,2] · Weijin Zhang[1,2,3] · Yang Yang[1,4] · Zhenhua Zeng[1,2] · Jianhua Wu[5] · Qin Zhang[1,2] · Yanan Liu[1] · Zhenfeng Chen[2] · Xiaohua Guo[2] · Ke-seng Zhao[2] · Qiaobing Huang[2] · Zhongqing Chen[1,2]

Received: 28 May 2019 / Revised: 30 August 2019 / Accepted: 23 September 2019 / Published online: 22 October 2019

Abstract

In a previous study, we demonstrated the role of polydatin (PD) in protecting against multiple organ dysfunction in sepsis. The aim of this study is to investigate whether PD protects against lipopolysaccharide (LPS)-induced endothelial barrier disruption through SIRT3 activation and to disclose the underlying mechanisms. Wild-type mice were injected with LPS and Evans Blue assay was performed to evaluate vascular permeability. Primary human umbilical vein endothelial cells (HUVECs) were stimulated with LPS. Endothelial permeability was evaluated by transendothelial electrical resistance (TER) and FITC-dextran leakage. SIRT3 activity was determined by a Deacetylase Fluorometric kit, and protein expression level of SIRT3 was detected by western blotting. Mitochondrial function was evaluated by determination of ROS level, mitochondrial membrane potential and mPTP opening. In endotoxemic mice, PD pretreatment attenuated vascular leakage in multiple organs while SIRT3 inhibition with 3-TYP reversed the effects of PD. PD treatment in late sepsis also exhibited barrier protective effects. In HUVECs, PD alleviated LPS-induced F-actin rearrangement, cadherin–catenin complex dissociation and endothelial hyperpermeability, whereas 3-TYP or SIRT3 siRNA attenuated the protective effects of PD. PD enhanced SIRT3 deacetylase activity, and attenuated LPS-induced decrease in SIRT3 expression as well. Furthermore, gain-of-function and loss-of-function strategies also confirmed the role of SIRT3 in enhancing endothelial barrier integrity. It was further ascertained that PD enhanced SIRT3-mediated deacetylation of SOD2 and cyclophilin D (CypD), thus suppressing mitochondrial dysfunction and subsequent endothelial barrier dysfunction. In addition, it was revealed that RAGE was involved in LPS-regulated SIRT3 signaling. Our results suggest that polydatin protects against LPS-induced endothelial barrier disruption dependent on SIRT3 and can be applied as a potential therapy for sepsis.

Introduction

Sepsis is a major health concern and is associated with high morbidity and mortality. Sepsis is usually triggered by a dysregulated host response to infection [1]. Recent studies showed that microvascular alteration and vascular leakage are associated with organ dysfunction and high mortality in sepsis [2, 3]. The endothelial barrier is maintained by adherens junctions (AJs), tight junctions (TJs) and their interactions with actomyosin cytoskeleton [4]. Vascular endothelial cadherin (VE-cadherin) is connected to actin

These authors contributed equally: Jie Wu, Zhiya Deng

✉ Qiaobing Huang
bing@smu.edu.cn

✉ Zhongqing Chen
zhongqingchen2008@163.com

[1] Department of Critical Care Medicine, Nanfang Hospital, Southern Medical University, Guangzhou 510515, China

[2] Guangdong Provincial Key Lab of Shock and Microcirculation, Department of Pathophysiology, Southern Medical University, Guangzhou 510515, China

[3] Department of Geriatrics, Shantou Central Hospital, Shantou 515000, China

[4] Department of Critical Care Medicine, the First People's Hospital of Chenzhou, Chenzhou 423000, China

[5] The First School of Clinical Medicine, Southern Medical University, Guangzhou 510515, China

cytoskeleton via several protein partners, including β-catenin, p120, and plakoglobin [5]. The stabilization of VE-cadherin-regulated AJs restores vascular barrier and reduces the mortality of septic mice [6], suggesting a promising therapeutic strategy targeting endothelial barrier function in sepsis.

Polydatin (PD), a traditional Chinese drug extracted from *Polygonum cuspidatum*, is an analog of resveratrol (RSV) with an additional β-D-glucose group. In a previous study, we identified PD as a new therapeutic agent for multiorgan dysfunction in sepsis [7]. Here, PD was found to exert a preventive effect on vascular leakage in multiple organs of endotoxemic mice (see "Results"). Importantly, the activating effect of PD on SIRT3 in hemorrhagic shock has been elucidated [8, 9]. Therefore, we wondered whether PD protects against LPS-induced endothelial hyperpermeability via SIRT3 activation.

SIRT3 is an NAD^+-dependent protein deacetylase that belongs to the silent information regulator 2 (SIR2) family. The targets of SIRT3 are involved in most of mitochondrial biological processes including ATP generation, reactive oxygen species (ROS) detoxification, electron transport chain function, mitochondrial permeability transition pore (mPTP) regulation and mitochondrial dynamics [10–12]. Recent studies have demonstrated the protective role of SIRT3 in the development of sepsis [8, 13, 14]. Zeng et al. revealed that SIRT3 can protect against pericyte loss and microvascular dysfunction in the lung of septic mice [15]. However, the underlying molecular mechanisms of SIRT3 in regulating endothelial barrier function in sepsis have not been fully elucidated.

The generation of ROS contributes to dissociation of VE-cadherin–β-catenin complex and leads to endothelial hyperpermeability [5]. SIRT3 detoxifies ROS by deacetylating a key mitochondrial antioxidant enzyme, manganese superoxide dismutase (SOD2) [9]. Therefore, we speculated that PD-activated SIRT3 might protect from LPS-disrupted endothelial barrier via deacetylating SOD2 and reducing ROS levels. Cyclophilin D (CypD) is the key component of mPTP and the acetylation of CypD leads to an increased susceptibility to mPTP opening [16]. We previously found that SIRT3-mediated CypD deacetylation suppressed mPTP opening and mitochondrial injury in severe hemorrhagic shock [17]. We wondered whether SIRT3-mediated CypD deacetylation also plays a role in PD-mediated endothelial barrier protection upon LPS stimulation.

Thus, we hypothesized that PD protects against LPS-induced endothelial barrier disruption via enhancing SIRT3-mediated deacetylation of SOD2 and CypD. This study aims to determine the role of PD in protection against LPS-induced endothelial hyperpermeability and the underlying mechanisms.

Materials and methods

Animal studies

Wild-type C57 mice (18–20 g) were acquired from the lab center of Southern Medical University. The protocol was approved by the Animal Care Committee of the Southern Medical University of China and was in accordance with the National Institutes of Health guidelines for ethical animal treatment. In exploration of the preventive effects of PD in LPS-induced endothelial barrier disruption, mice were divided into four groups, the saline group, LPS group, PD + LPS group, and PD + LPS + 3-TYP group. Mice in LPS group were applied with 15 mg/kg LPS via intraperitoneal injection. Mice in PD + LPS group were applied with 30 mg/kg PD via tail vein injection 2 h prior to LPS injection. Mice in PD + LPS + 3-TYP group were applied with 30 mg/kg PD plus 5 mg/kg 3-TYP via tail vein injection 2 h prior to LPS injection. After 6 h of LPS application, 200 μL of 0.5% Evans Blue dye was injected through tail vein. While in exploration of the therapeutic effects of PD on endothelial barrier function in later sepsis, mice were divided into three groups, the saline group, LPS group, and LPS + PD group. Mice in LPS + PD group were applied with LPS injection followed by PD application (30 mg/kg) via tail vein injection at 18 h. After 24 h of LPS application, 200 μL of 0.5% Evans Blue dye was injected through tail vein. Then, the mice were sacrificed through cervical dislocation 30 min later. Via heart puncture, the mice were perfused with PBS + 2 mM EDTA for 20 min. The lung, kidney, liver, and small intestine were harvested and incubated in formamide at 55 °C for 2 days to elute the Evans Blue dye. The optical density (OD) of the formamide solution was determined at 620 nm using a Microplate Reader (SpectraMax M5).

Cells and reagents

Primary human umbilical vein endothelial cells (HUVECs), ECM medium, fetal bovine serum (FBS), penicillin and streptomycin were obtained from Sciencell (Carlsbad, CA, USA). HUVECs harvested between the second and sixth passage were applied in the experiments. Trypsin was supplied by Gibco BRL (Grand Island, NY, USA). LPS was acquired from Sigma (St. Louis, MO, USA). PD was supplied by Shenzhen Neptunus Pharmaceutical Co., Ltd. SIRT3 inhibitor 3-TYP was synthesized and characterized by the School of Pharmaceutical Sciences at Southern Medical University based on the work of Pi et al. [18]. Antibody against SIRT3 (sc-365175) was purchased from Santa Cruz Biotechnology (Santa Cruz, CA, USA). Antibodies targeting β-catenin (ab32572), VE-cadherin (ab33168), and CypD (ab110324) were acquired from Abcam (USA). Antibodies recognizing SOD2 (A1340),

SIRT1 (A0127), and pan acetylated lysine (A2391) were purchased from Abclonal (China). Rabbit IgG antibody (B900610) and mouse IgG antibody (B900620) were purchased from Proteintech (USA). Antibody against RAGE (MAB-11451-100) was acquired from R&D systems (Minneapolis, MN, USA) and at 10 μg/mL, this antibody will block 90% of RAGE binding. Antibody against GAPDH (5174) was acquired from CST (Danvers, MA, USA).

Detection of SIRT1/3 activity

SIRT1/3 deacetylase activity was detected using SIRT1 (Cyclex, Cat#CY-1151V2) and SIRT3 (Cyclex, Cat#CY-1153V2) Deacetylase Fluorometric Assay kits as described previously [19]. Briefly, cells were lysed and immunoprecipitated with SIRT1/3 antibody. The final mixture contained 50 mM Tris-HCl (pH 8.8), 4 mM $MgCl_2$, 0.5 mM DTT, 0.25 mA/mL lysyl endopeptidase, 1 μM trichostatin A, 200 μM NAD^+, and 5 μL extraction buffer. Fluorescence intensity was determined at 350 nm/450 nm by Automatic Microplate Reader (Molecular Devices, Sunnyvale, CA, USA).

Detection of SOD2 activity

The activity of SOD2 was determined using a commercially available kit (Dojindo Molecular Technology, Kumamoto, Japan). Briefly, total SOD activity of the immunoprecipitated proteins was measured by inhibition rate of water-soluble tetrazolium salt (WST-1) reduction. Potassium cyanide was added to the lysate during the assay to inhibit both SOD1 and SOD3. Absorbance was determined at 450 nm using a Microplate Reader (SpectraMax M5). SOD2 activity was calculated as a rate of inhibition at which 1 U was defined as a 50% decrease from the control value over a period of 30 min at 37 °C.

Western blotting

Protein extracted from HUVECs were separated by SDS-PAGE and then transferred to the polyvinylidene fluoride membranes. Blots were incubated with 5% bovine serum albumin (BSA) to block nonspecific site for 1 h and then incubated overnight at 4 °C with primary antibodies of SIRT3, β-catenin, VE-cadherin, SOD2, and CypD at 1:1000. Afterwards, they were incubated with a secondary antibody for 1 h and signals were measured using chemiluminescence reagents (Pierce, USA).

Transfection of siRNA

HUVECs were grown in antibiotic-free ECM in culture dishes for 24 h and were transfected with target siRNA using Lipofectamine 2000 according to the manufacturer's instructions. The sequences of oligonucleotide for control, SIRT3, SOD2 and CypD siRNA were synthesized by GenePharma (Shanghai, China). The siRNA-targeted sequences were as follows: control siRNA, sense 5′-UUCUCCGAACGUGUCACGUTT-3′ and antisense 5′-ACGUGACACGUUCGGAGAATT-3′; SIRT3 siRNA, sense 5′-GGUGGAAGAAGGUCCAUAUtt-3′ and antisense 5′-AUAUGGACCUUCUUCCACCtt-3′; SOD2 siRNA, sense 5′- GCAUCUGUUGGUGUCCAAGTT-3′ and antisense 5′-CUUGGACACCAACAGAUGCTT-3′; CypD siRNA, sense 5′-UUUGACGUGACCGAACACAACAUGC-3′ and antisense 5′-GCAUGUUGUGUUCGGUCACGUCAAA-3′. Forty-eight hours after transfection, the cells were collected and processed for following experiments.

Adenoviral infection

The adenoviral vector expressing flag- and GFP-tagged SIRT3 (Ad-SIRT3) and empty vector (Ad-GFP) were packaged by GeneChem Co. Ltd (Shanghai, China). Cells were infected with the adenoviruses for 48 h, followed by corresponding experiments.

Immunofluorescent staining of F-actin

HUVECs were plated in Petri dishes and subjected to different treatments. Cells were washed with PBS three times, and then were fixed with 3.7% formaldehyde and perforated with 0.5% Triton X-100. Then, cells were blocked with 5% BSA for 1 h, followed by incubation with rhodamine phalloidin at room temperature for 1 h. Finally, cells were washed with PBS three times and subsequently detected with a confocal scanning microscope (Zeiss, Germany).

Co-immunoprecipitation (Co-IP) assays

HUVEC lysate was harvested, and Co-IP assay was performed using an Immunoprecipitation kit from Proteintech (Chicago, IL, USA). Briefly, 2 μg of antibodies against the proteins of interest or a negative control IgG of the same species were added to the cell lysate. Then the IP buffer was mixed with protein A/G beads. The immunoprecipitate was separated by SDS–PAGE and analyzed by western blot.

Measurement of ROS level

Level of intracellular ROS was assessed with Dichlorofluorescein diacetate (DCFH-DA) from Sigma (USA). Briefly, HUVECs were incubated with 10 μM DCFH-DA in dark at 37 °C for 30 min, then washed for three times with PBS. Fluorescence intensity of each sample was detected through a confocal scanning microscope (Zeiss, Germany). Mitochondrial ROS level was detected using the MitoSOX Red (Invitrogen). Cells were incubated with 5 μM MitoSOX Red reagent in dark at 37 °C for 10 min. Cells were washed

gently three times with PBS. Mitochondrial ROS level was then determined by the fluorescence intensity.

Determination of transendothelial electrical resistance

Transendothelial electrical resistance (TER) of HUVEC monolayer was determined by STX2 electrode and EVOM^2 meter according to the manufacturer's protocol (World Precision Instruments, USA) [20]. Briefly, 200 µL of HUVECs at 10^5/mL were seeded onto the transwell upper chamber and grown to confluence. Resistance values of multiple transwell inserts of the experimental group were sequentially measured and the mean was expressed in the common unit (Ω cm^2) after the value of a blank cell-free filter was subtracted.

Dextran transendothelial flux

As previously described [21], HUVECs were grown to confluence on transwell membranes and tracer FITC-labeled dextran (1 mg/mL) was added to the upper chambers for 45 min. Samples were then collected from upper and lower chambers. The concentrations of dextran were determined with a HTS 7000 microplate reader. The permeability of endothelial monolayer was evaluated as permeability coefficient of dextran (Pd) calculated as follows: $Pd = [A]/t \times 1/A \times V/[L]$, where $[A]$ is the dextran concentration in bottom chamber, t is time in seconds, A indicates the membrane area in cm^2, V is the bottom chamber volume and $[L]$ is the concentration of dextran in the upper chamber.

Mitochondrial membrane potential assay

Mitochondrial membrane potential (ΔΨm) was measured by monitoring fluorescence aggregates of JC-1 from Molecular Probes (Eugene, OR, USA) as previously described [8]. The formation of JC-1 monomers and their fluorescence linearly correlated to decrease in membrane potential. Briefly, HUVECs were incubated with JC-1 at 37 °C for 15 min. Afterwards, the cells were washed three times with PBS and a fluorescence microscope was used to detect the mitochondrial membrane potential.

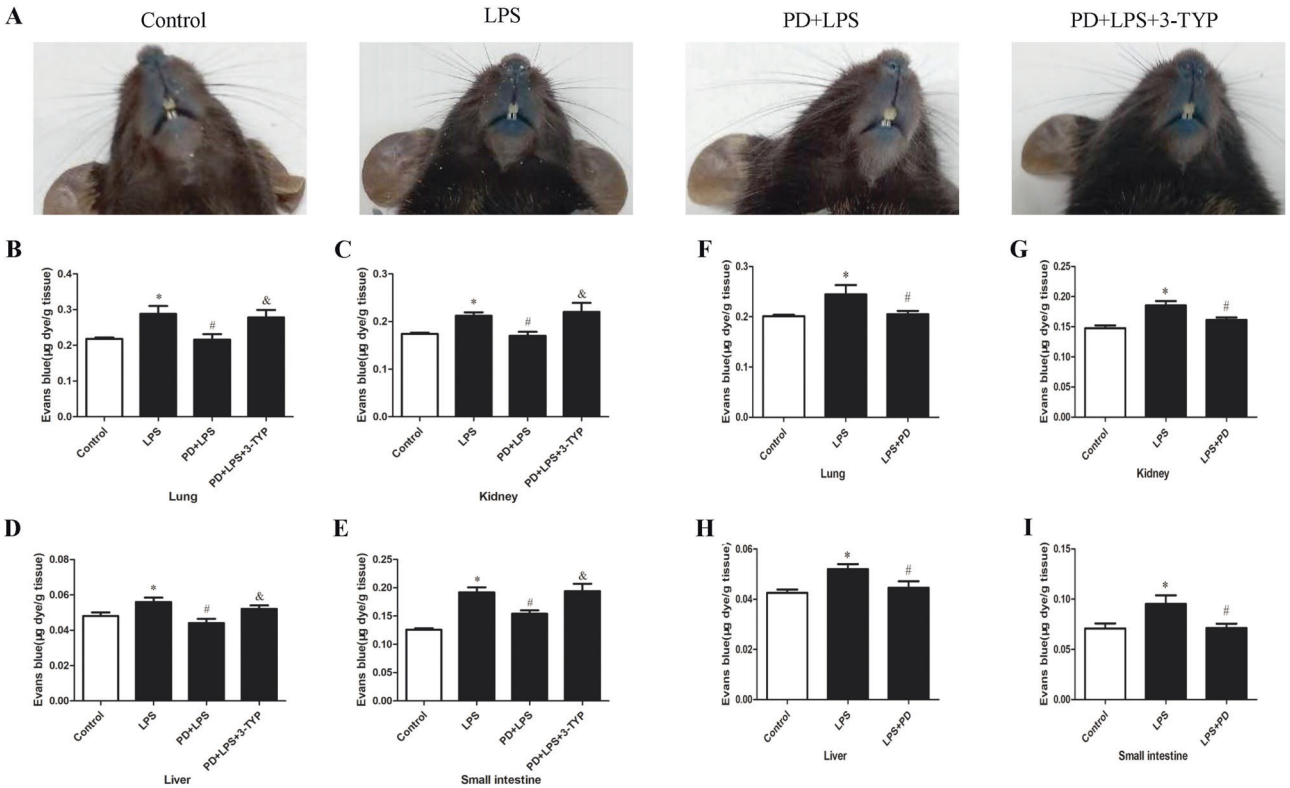

Fig. 1 PD mediated protective effects in LPS-elicited vascular leakage via SIRT3 activation. Mice were pretreated with PD (30 mg/kg) or PD (30 mg/kg) plus 3-TYP (5 mg/kg) or saline via tail vein injection for 2 h, then were injected with 15 mg/kg LPS intraperitoneally for 6 h. **a** Representative pictures of mouse skin were taken 30 min after Evans Blue injection. **b–e** Quantitative analysis of vascular permeability using Evans Blue and expressed as µg of dye per g of tissue. Vascular permeability was evaluated in the lung (**b**), kidney (**c**), liver (**d**) and small intestine (**e**). $n = 5$. $^*P < 0.05$ versus control, $^\#P < 0.05$ versus LPS, $^\&P < 0.05$ versus PD + LPS. Mice were injected with 15 mg/kg LPS intraperitoneally for 24 h, with PD (30 mg/kg) or saline administration via tail vein injection at 18 h. **f–i**, Quantitative analysis of vascular permeability using Evans Blue and expressed as µg of dye per g of tissue. Vascular permeability was evaluated in the lung (**f**), kidney (**g**), liver (**h**), and small intestine (**i**). $n = 5$. $^*P < 0.05$ versus control, $^\#P < 0.05$ versus LPS

The mPTP opening assay

The opening of mPTP was determined by calcein-AM from Molecular Probes (Eugene, OR, USA). All procedures completely complied with the manufacture's instructions. In brief, HUVECs were loaded with 1 μmol/L calcein-AM at 37 °C for 20 min, followed by incubation with 1 mmol/L $CoCl_2$ to quench cytosolic and nuclear fluorescence at room temperature for 15 min. The fluorescence was observed by a fluorescence microscope.

Statistical analysis

Data was expressed as mean ± SE of at least three independent experiments and analyzed using SPSS 16.0 software version. Statistical comparisons were performed using a one-way analysis of variance followed by post hoc pairwise comparisons. $P < 0.05$ was considered significant.

Results

Effect of PD on LPS-induced endothelial barrier disruption

Previously, we investigated the efficacy of PD in the treatment of sepsis. We found that PD (30 mg/kg) improved the survival rate from 26.7 to 50% in cecal ligation and puncture-induced septic rats [22]. Given the important role of endothelial barrier dysfunction in the development of sepsis, here, we further explored the barrier protective effects of PD in sepsis. Evans Blue assay was performed to determine alterations in vascular permeability in endotoxemic mice at 6 h after LPS administration. On oral and maxillofacial skin of the mice, it was observed that LPS caused significant leakage of Evans Blue dye. Pretreatment of PD ameliorated LPS-induced vascular leakage significantly (Fig. 1a). Furthermore, quantification of Evans Blue dye leakage in lung, kidney, liver, and small intestine showed similar alterations in vascular permeability (Fig. 1b–e). To further reveal the therapeutic effect of PD on barrier protection in late sepsis, we observed organ edema by detecting Evans Blue leakage in mice 24 h after LPS treatment with PD administration at 18 h. It was found that PD treatment at late sepsis also attenuated vascular leakage in lung, kidney, liver, and small intestine as well (Fig. 1f–i). In LPS-treated endothelial cells, PD reversed LPS-induced F-actin redistribution and cadherin–catenin complex dissociation (Fig. 2a, b). As we previously demonstrated, LPS induced endothelial monolayer hyperpermeability in a time-dependent manner [20]. In present study, PD attenuated LPS-induced decrease in TER value and increase in FITC-dextran leakage (Fig. 2c, d). Altogether, these results show that PD exerts protective effects against LPS-induced vascular barrier disruption.

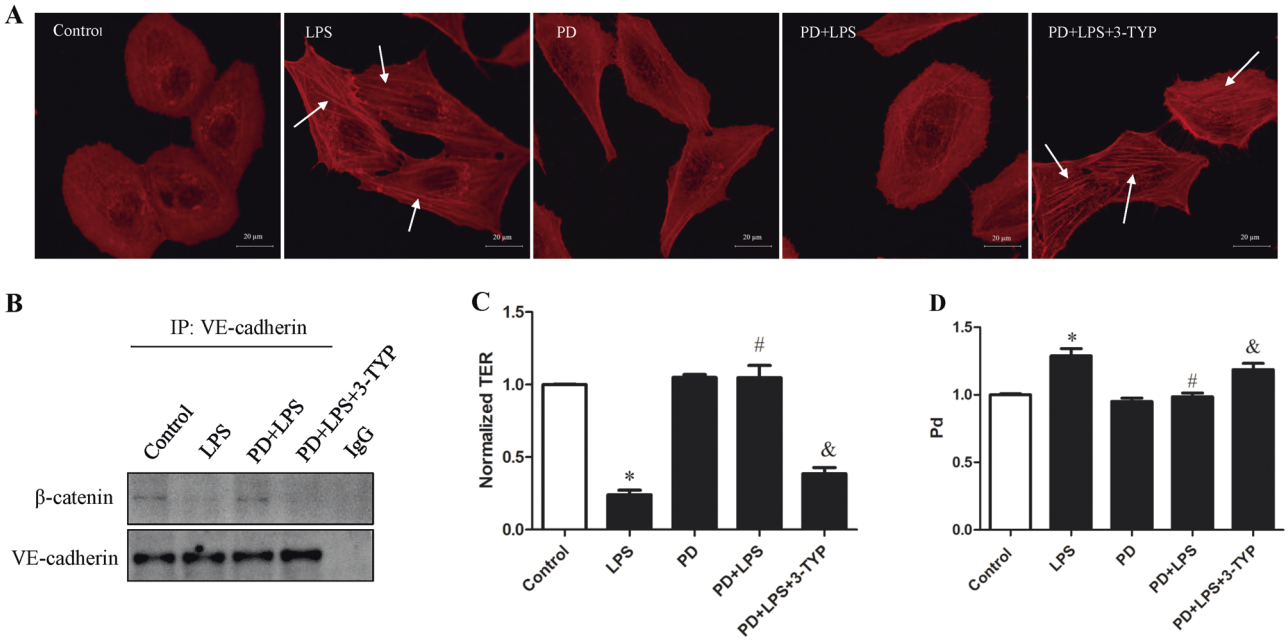

Fig. 2 PD mediated protective effects in LPS-induced endothelial hyperpermeability via SIRT3 activation. HUVECs were pretreated with PD (50 μM) or PD (50 μM) plus 3-TYP (50 μM) for 2 h, then were treated with 1 μg/mL LPS or PBS for 12 h. **a** Distribution of F-actin in the cytoskeleton was examined using confocal microscopy and actin filaments were marked with white arrows. **b** Whole cell lysates were prepared and probed in co-immunoprecipitation assays with an anti-VE-cadherin antibody. Western blot assays were then performed for the immunoprecipitated samples with an anti-β-catenin antibody. **c, d** HUVECs were pretreated with PD (50 μM) or PD (50 μM) plus 3-TYP (50 μM) for 2 h, then were treated with 1 μg/mL LPS or PBS for 24 h. Endothelial monolayer permeability was assessed by TER (**c**) and flux of FITC-dextran (**d**). $n = 3$. $^{*}P < 0.05$ versus control, $^{\#}P < 0.05$ versus LPS, $^{\&}P < 0.05$ versus PD + LPS

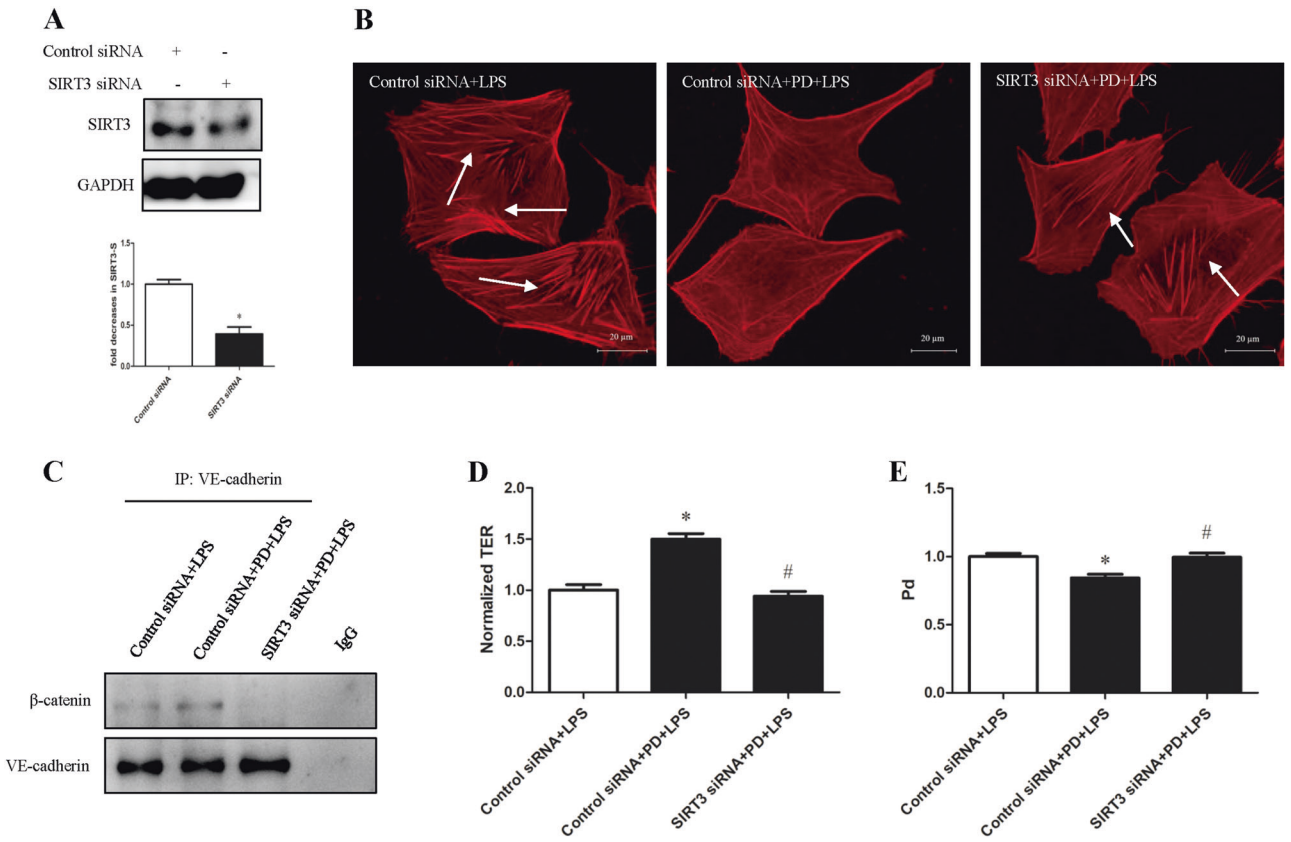

Fig. 3 SIRT3 deletion abrogated PD-mediated endothelial barrier protection. HUVECs were transfected with either control siRNA or SIRT3 siRNA. **a** Protein expression levels of SIRT3 were measured by western blot analysis. Transfected HUVECs were pretreated with PD (50 μM) for 2 h, then followed by LPS (1 μg/mL) treatment for 12 h. **b** Distribution of F-actin in the cytoskeleton was examined using confocal microscopy and actin filaments were marked with white arrows. **c** Whole cell lysates were prepared and probed in co-immunoprecipitation assays with an anti-VE-cadherin antibody. Western blot assays were then performed for the immunoprecipitated samples with an anti-β-catenin antibody. **d, e** Endothelial monolayer permeability was assessed by TER (**d**) and flux of FITC-dextran (**e**). $n = 3$. $^{*}P < 0.05$ versus control siRNA + LPS, $^{\#}P < 0.05$ versus control siRNA + PD + LPS

PD attenuates LPS-induced SIRT3 downregulation in endothelial cells

It has been reported that SIRT3 is involved in the regulation of endothelial permeability [23]. Importantly, we have previously demonstrated that PD can act as an agonist of SIRT3 [7–9]. To determine whether SIRT3 plays a role in PD-exerted barrier protective effects, the deacetylase activity and protein expression of SIRT3 were studied. As shown in Fig. 3a, LPS induced a significant decrease in SIRT3 activity over time. Consistent with our previous findings, PD enhanced SIRT3 deacetylase activity significantly (Fig. 3b). The expression of SIRT3 protein was decreased from 12 to 24 h in response to LPS stimulation (Fig. 3d). Moreover, we found that PD alleviated LPS-induced decrease in SIRT3 expression (Fig. 3e). These results suggest that PD may prevent LPS-induced endothelial barrier disruption by upregulating the SIRT3 activity and expression.

SIRT3 inhibition eliminates the barrier protective effects of PD

SIRT3 specific inhibitor 3-TYP was used and the inhibiting effect of 3-TYP was confirmed (Fig. 3b). To verify the specificity of 3-TYP, SIRT1 activity was examined and there was no significant difference (Fig. 3c). 3-TYP reversed PD-mitigated decrease in SIRT3 expression caused by LPS (Fig. 3e). Moreover, 3-TYP abrogated the barrier protective effect of PD in multiple organs of septic mice (Fig. 1). In HUVECs, 3-TYP diminished PD-mediated protection against F-actin redistribution, cadherin–catenin complex dissociation, and endothelial monolayer hyperpermeability (Fig. 2a–d). We applied SIRT3 siRNA to further confirm the role of SIRT3 in PD-mediated endothelial barrier protection. Not surprisingly, SIRT3 knockdown abrogated PD-mitigated F-actin redistribution, cadherin–catenin complex dissociation, and endothelial monolayer hyperpermeability (Fig. 4a–d). These results

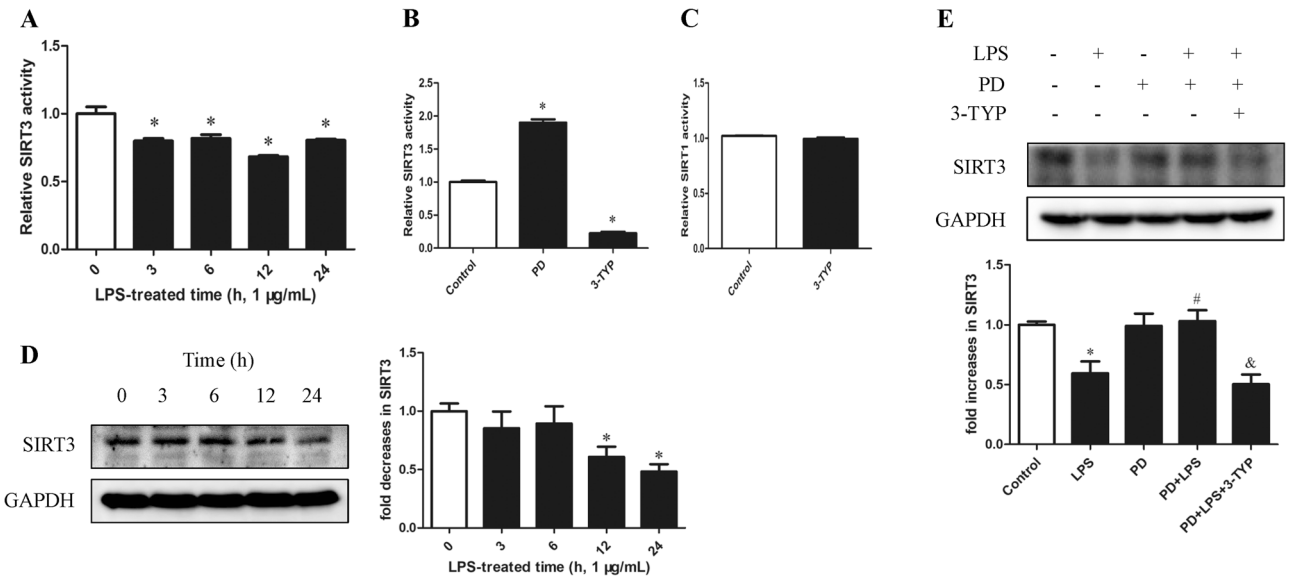

Fig. 4 Effect of PD on alterations of SIRT3 activity and protein expression in response to LPS challenge. HUVECs were exposed to 1 μg/mL LPS for the indicated times. **a** SIRT3 activity was determined using a SIRT3 Assay kit. $n = 3$. $^{*}P < 0.05$ versus 0 h. **b** SIRT3 activity was examined and PD enhanced SIRT3 activity, while 3-TYP inhibited SIRT3 activity. $n = 3$. $^{*}P < 0.05$ versus control. **c** SIRT1 activity was examined and 3-TYP showed no effect on SIRT1 activity. $n = 3$. **d** Protein expression levels of SIRT3 were detected by western blot analysis. $n = 3$. $^{*}P < 0.05$ versus 0 h. **e** HUVECs were pretreated with PD (50 μM) or PD (50 μM) plus 3-TYP (50 μM) for 2 h, then were treated with 1 μg/mL LPS or PBS for 12 h. Protein expression levels of SIRT3 were detected by western blot analysis. $n = 3$. $^{*}P < 0.05$ versus control, $^{\#}P < 0.05$ versus LPS, $^{\&}P < 0.05$ versus PD + LPS

indicate that PD attenuates LPS-elicited vascular barrier disruption through SIRT3 activation.

Role of SIRT3 in LPS-induced endothelial barrier disruption

Here, the gain-of-function and loss-of-function approaches were used to confirm the protective role of SIRT3 activation in LPS-induced barrier disruption. The infection efficiency of an adenovirus overexpressing SIRT3 was observed with GFP and SIRT3 expression (Fig. 5a, b). As expected, overexpressed SIRT3 reversed LPS-induced F-actin rearrangement, cadherin–catenin complex dissociation, and endothelial hyperpermeability (Fig. 5d–g), mimicking PD-mediated barrier protection. In contrast to SIRT3 overexpression, SIRT3 siRNA exacerbated LPS-induced F-actin redistribution, cadherin–catenin complex dissociation, and endothelial hyperpermeability (Fig. 6c–f). These results fully confirm the protective role of SIRT3 in LPS-mediated endothelial hyperpermeability.

PD protects endothelial barrier integrity via SIRT3-SOD2-ROS signaling

Mounting evidence suggest that SIRT3 can deacetylate and subsequent activate SOD2, thus promoting ROS clearance [24–26]. We wondered if SIRT3–SOD2–ROS signaling mediates the protective effects of PD on LPS-induced endothelial barrier dysfunction. Results in this study showed that LPS elicited a significant increase in SOD2 acetylation, as well as decrease in activity. PD pretreatment inhibited LPS-mediated alterations of SOD2 acetylation and activity levels (Fig. 7a, b). Consistently, PD strongly attenuated LPS-induced cellular and mitochondrial ROS generation and MDA increase (Fig. 7c–e). SIRT3 overexpression mimicked PD-mediated protection against LPS-induced mitochondrial ROS generation (Fig. 5c). However, the protective effects of PD were abolished by SIRT3 inhibition with 3-TYP (Fig. 7c–e). Similarly, SIRT3 knockdown intensified LPS-evoked cellular and mitochondrial ROS generation (Fig. 6a, b).

Given that mito-TEMPO, a mitochondrially targeted antioxidant, can enhance SOD2 activity and thus suppress ROS generation [27], we applied it for the following experiments. Results showed that mito-TEMPO ameliorated LPS-induced elevation in endothelial permeability, while 3-TYP reversed the effect of mito-TEMPO (Fig. 7f, g). To further confirm the role of SIRT3–SOD2–ROS axis, SOD2 siRNA was used. The efficiency of SOD2 siRNA transfection was verified in Fig. 7h. As expected, SOD2 knockdown abolished SIRT3 overexpression-mediated barrier protection (Fig. 7i–j). The above results suggest that PD prevents LPS-induced endothelial barrier disruption through SIRT3–SOD2–ROS axis.

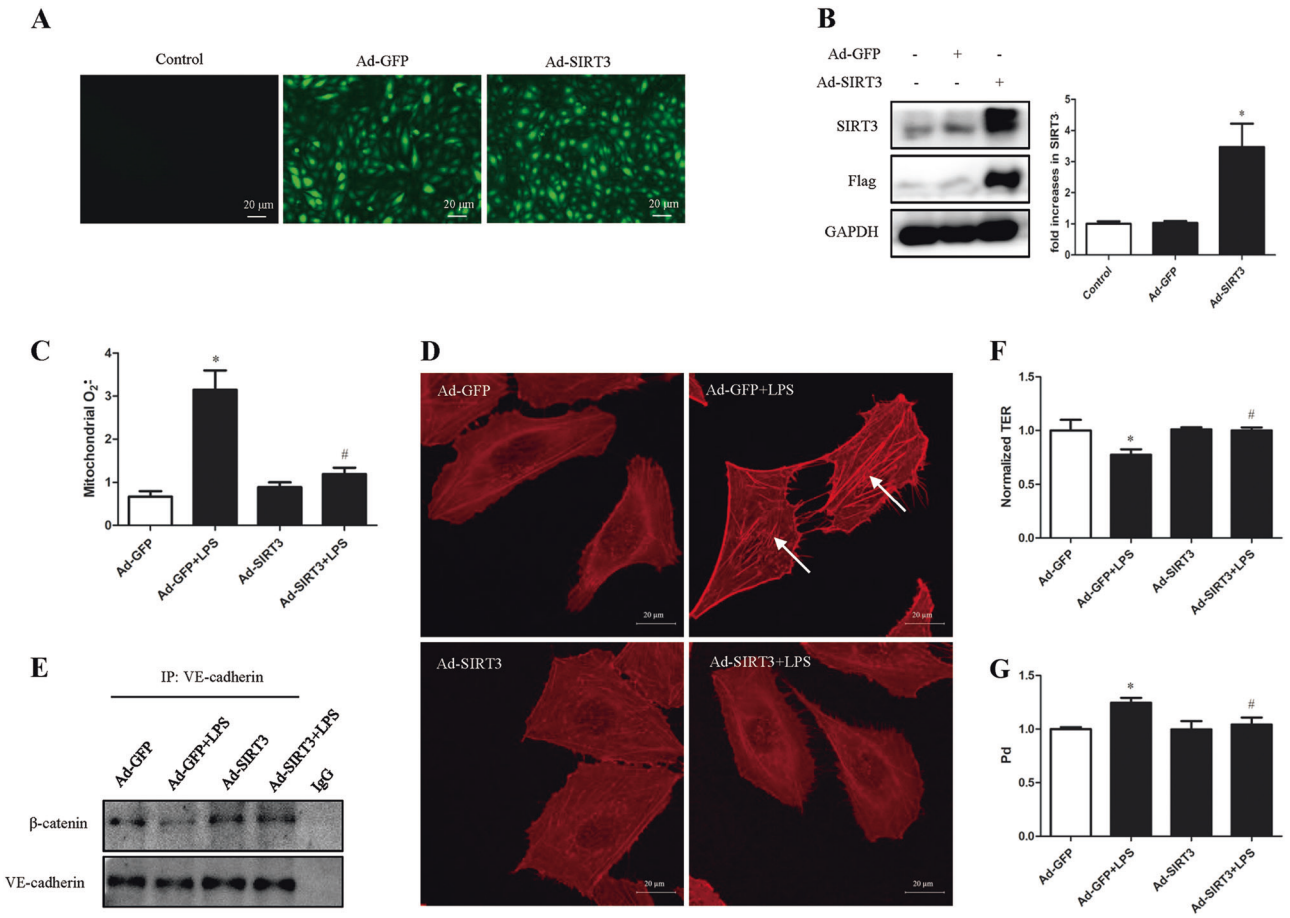

Fig. 5 Overexpression of SIRT3 reversed LPS-induced ROS generation and endothelial hyperpermeability. HUVECs were infected with empty adenovirus vector (Ad-GFP) or adenovirus containing flag- and GFP-labeled SIRT3 (Ad-SIRT3) for 48 h. **a** Adenovirus infection efficiency was identified by GFP expression using a fluorescent microscope. **b** Western blot was used to examine the endogenous and induced SIRT3 levels. Infected HUVECs were treated with LPS (1 μg/mL) or PBS for 12 h. **c** Mitochondrial $O_2^{\bullet -}$ were measured by MitoSOX. **d** Distribution of F-actin in the cytoskeleton was examined using confocal microscopy and actin filaments were marked with white arrows. **e** Whole cell lysates were prepared and probed in co-immunoprecipitation assays with an anti-VE-cadherin antibody. Western blot assays were then performed for the immunoprecipitated samples with an anti-β-catenin antibody. **f–g** Infected HUVECs were treated with LPS (1 μg/mL) or PBS for 24 h. Endothelial monolayer permeability was assessed by TER (**f**) and flux of FITC-dextran (**g**). $n = 3$. $^{*}P < 0.05$ versus control or Ad-GFP, $^{\#}P < 0.05$ versus Ad-GFP + LPS

PD protects endothelial barrier function through SIRT3-mediated CypD deacetylation

CypD, a key regulator of the mitochondrial mPTP, is deacetylated by SIRT3, thereby reducing mPTP susceptibility and maintaining mitochondrial function [16, 28]. To determine whether SIRT3-mediated CypD deacetylation is involved in PD-exerted protective effects upon LPS-induced endothelial barrier disruption, acetylation level of CypD was examined. As shown in Fig. 8a, introduction of LPS led to increased CypD acetylation, which was ameliorated by PD pretreatment. However, the effect of PD on LPS-induced CypD acetylation was abolished by SIRT3 inhibitor 3-TYP. In addition, Co-IP analysis revealed that PD pretreatment diminished LPS-elicited dissociation of CypD from SIRT3, while 3-TYP abrogated the effect of PD (Fig. 8b). The mitochondrial membrane potential (ΔΨm) and mPTP were then investigated via JC-1 staining and calcein-AM followed by $CoCl_2$ quenching, respectively. Results showed that LPS treatment caused mPTP opening and loss of ΔΨm, which were attenuated by PD pretreatment. However, 3-TYP abolished the effects of PD on LPS-mediated alterations of ΔΨm and mPTP (Fig. 8c, d). CypD knockdown was then performed and efficiency of CypD siRNA was confirmed through western blotting (Fig. 8e). As shown in Fig. 8f, g, CypD knockdown ameliorated LPS-induced endothelial barrier disruption significantly. Taken together, these results indicate that PD alleviates LPS-induced barrier disruption through SIRT3-mediated deacetylation of CypD and suppression of mPTP opening.

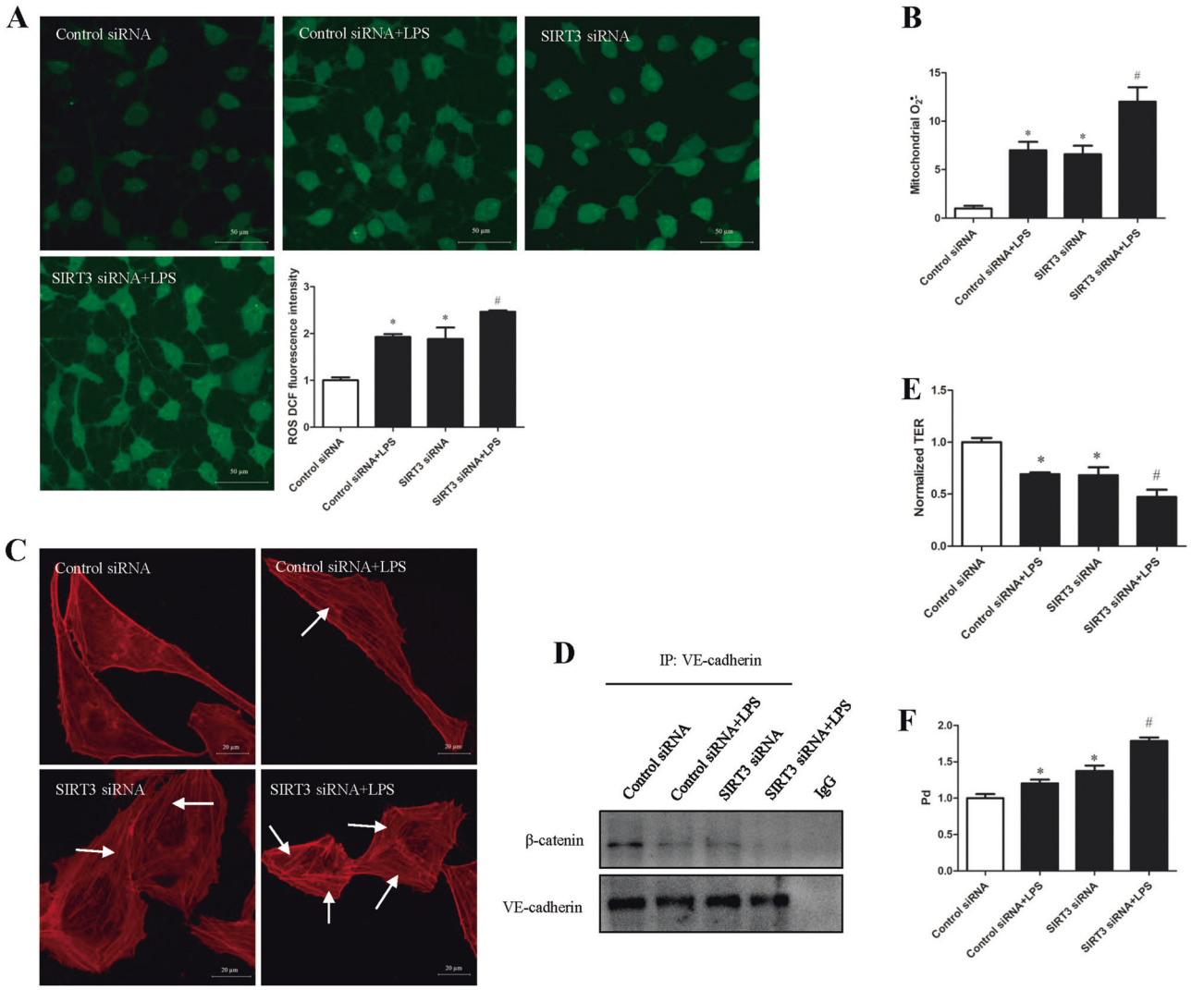

Fig. 6 SIRT3 ablation exacerbated LPS-mediated ROS generation and endothelial hyperpermeability. HUVECs were transfected with either control siRNA or SIRT3 siRNA. Transfected HUVECs were stimulated with LPS (1 μg/mL) or PBS for 12 h. **a** Representative images and quantification of intracellular ROS formation were measured by DCFH-DA. **b** Mitochondrial $O_2^{\bullet -}$ were measured by MitoSOX. **c** Distribution of F-actin in the cytoskeleton was examined using confocal microscopy and actin filaments were marked with white arrows. **d** Whole cell lysates were prepared and probed in co-immunoprecipitation assays with an anti-VE-cadherin antibody. Western blot assays were then performed for the immunoprecipitated samples with an anti-β-catenin antibody. **e**, **f** Transfected HUVECs were stimulated with LPS (1 μg/mL) or PBS for 24 h. Endothelial monolayer permeability was assessed by TER (**e**) and flux of FITC-dextran (**f**). $n = 3$. $^{*}P < 0.05$ versus control siRNA, $^{\#}P < 0.05$ versus control siRNA + LPS or SIRT3 siRNA

Role of RAGE in LPS-regulated SIRT3 activity and protein expression

A previous study revealed that RAGE was involved in advanced glycation end product (AGE)-induced decrease in SIRT3 expression in endothelial progenitor cells (EPCs) [29]. We have demonstrated that RAGE is involved in LPS-elicited endothelial hyperpermeability [20]. To investigate whether RAGE has effect on alteration of SIRT3 signaling in response to LPS treatment, RAGE blocking antibody was used. Results showed that RAGE antibody alleviated LPS-induced decrease in SIRT3 deacetylase activity (Fig. 9a). Intriguingly, RAGE antibody was able to diminish LPS-reduced protein expression of SIRT3 as well (Fig. 9b). Therefore, it is clearly suggested that RAGE is involved in LPS-induced endothelial barrier disruption via regulating SIRT3 signaling pathways.

Discussion

The disruption of endothelial barrier in sepsis could dispose to vascular leak, shock, and organ failure. Considerable evidences suggest that SIRT3 has a protective role in the

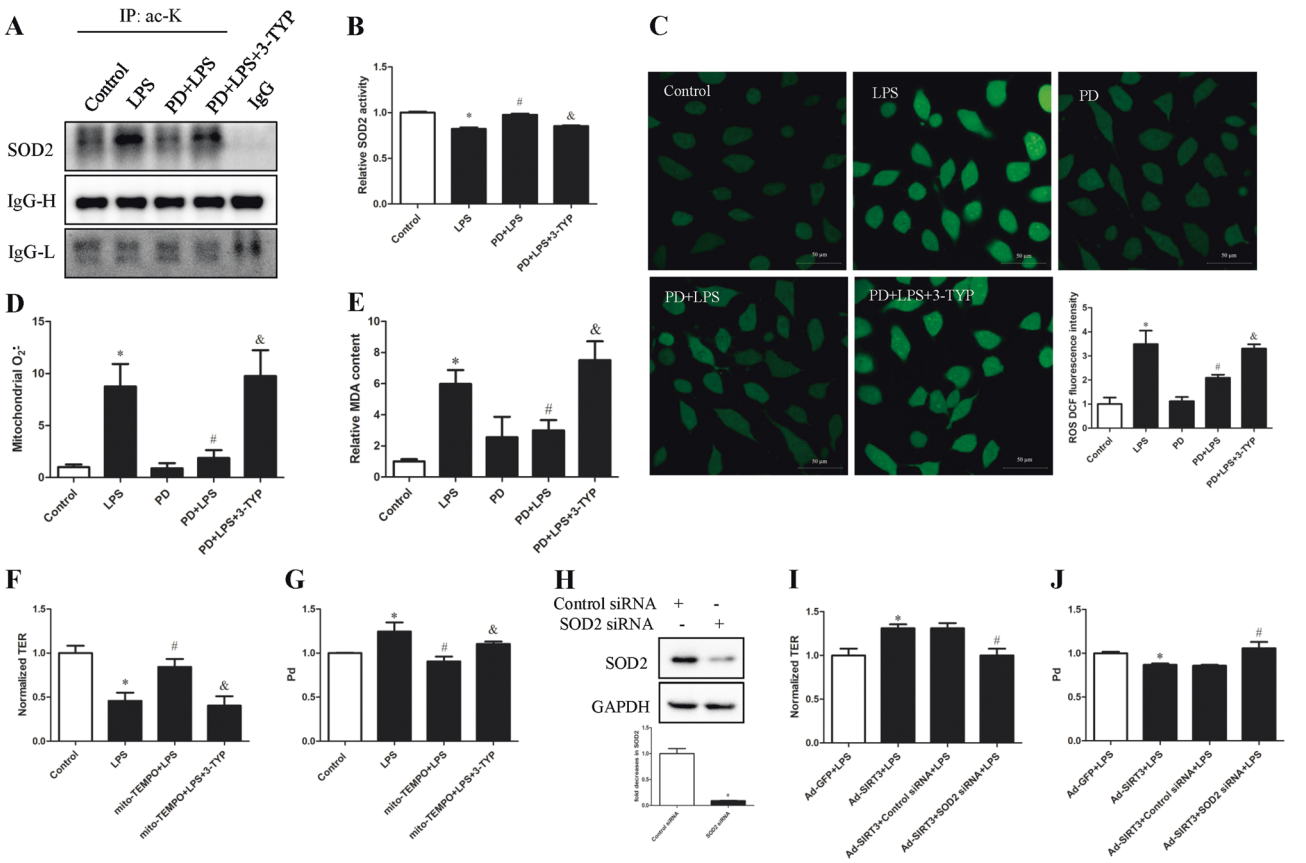

Fig. 7 Role of SIRT3-SOD2-ROS axis in PD-mediated barrier protective effects. HUVECs were pretreated with PD (50 μM) or PD (50 μM) plus 3-TYP (50 μM) for 2 h, then cells were treated with 1 μg/mL LPS for 12 h. **a** Whole cell lysates were prepared and probed in co-immunoprecipitation assays with a pan acetyl-lysine antibody. Western blot assays were then performed for the immunoprecipitated samples with an anti-SOD2 antibody. **b** SOD2 activity was determined based on an enzymatic reaction using an SOD2 Assay kit. **c** Representative images and quantification of intracellular ROS formation were measured by DCFH-DA. **d** Mitochondrial $O_2^{\bullet -}$ were measured by MitoSOX. **e** The lipid peroxidation levels of HUVECs were measured by MDA assay. $n = 3$. $^{*}P < 0.05$ versus control, $^{\#}P < 0.05$ versus LPS, $^{\&}P < 0.05$ versus PD + LPS. **f–g** HUVECs were pretreated with mito-TEMPO (1 μM) or mito-TEMPO (1 μM) plus 3-TYP (50 μM) for 2 h, followed by stimulation with 1 μg/mL LPS for 24 h. Endothelial monolayer permeability was assessed by TER (**f**) and flux of FITC-dextran (**g**). $n = 3$. $^{*}P < 0.05$ versus control, $^{\#}P < 0.05$ versus LPS, $^{\&}P < 0.05$ versus mito-TEMPO + LPS. **h** HUVECs were transfected with either control siRNA or SOD2 siRNA. Protein expression levels of SOD2 were measured by western blot analysis. $n = 3$. $^{*}P < 0.05$ versus control siRNA. **i–j** Transfected HUVECs were infected with control or SOD2 siRNA, and then treated with LPS (1 μg/mL) for 24 h. Endothelial monolayer permeability was assessed by TER (**i**) and flux of FITC-dextran (**j**). $n = 3$. $^{*}P < 0.05$ versus Ad-GFP + LPS, $^{\#}P < 0.05$ versus Ad-SIRT3 + SOD2 siRNA + LPS

pathogenesis of sepsis [13, 30, 31]. In present study, we show that PD prevents LPS-induced endothelial barrier disruption in endotoxemic mice and endothelial cells via SIRT3 activation. Through deacetylation of mitochondrial SOD2 and CypD, PD-mediated SIRT3 activation preserved mitochondrial functions, thus reversing LPS-elicited endothelial hyperpermeability. In addition, RAGE was identified as a negative regulator of SIRT3 activity and protein expression in response to LPS challenge.

Apart from PD, several drugs have been reported to activate SIRT3, including RSV [23], honokiol [32], and melatonin [33]. However, no specific agonist for SIRT3 has been found. It should not be neglected that PD can also activate SIRT1 [34]. Notably, SIRT3 and SIRT1 have been found to have redundant effects on protecting cells in some stress conditions. However, it was confirmed that the inhibitor 3-TYP specifically inhibits SIRT3 without affecting SIRT1, which is consistent with our previous study [9]. And we also used SIRT3 knockdown approach to confirm the role of SIRT3 in PD-mediated barrier protection.

Regulation of endothelial permeability is a complex process involving signaling components that are associated with AJs, TJs, and cytoskeletal proteins. AJs are composed of VE-cadherin and its intracellular partners. Cell-adhesive activity is enhanced by the interaction between VE-cadherin and β-catenin or plakoglobin, which in turn bind to α-catenin [35]. The disruption of junctional assembly of VE-cadherin and β-catenin is one of the key mechanisms leading to microvascular hyperpermeability [36]. Here, it was proved that PD-activated SIRT3 contributed to the

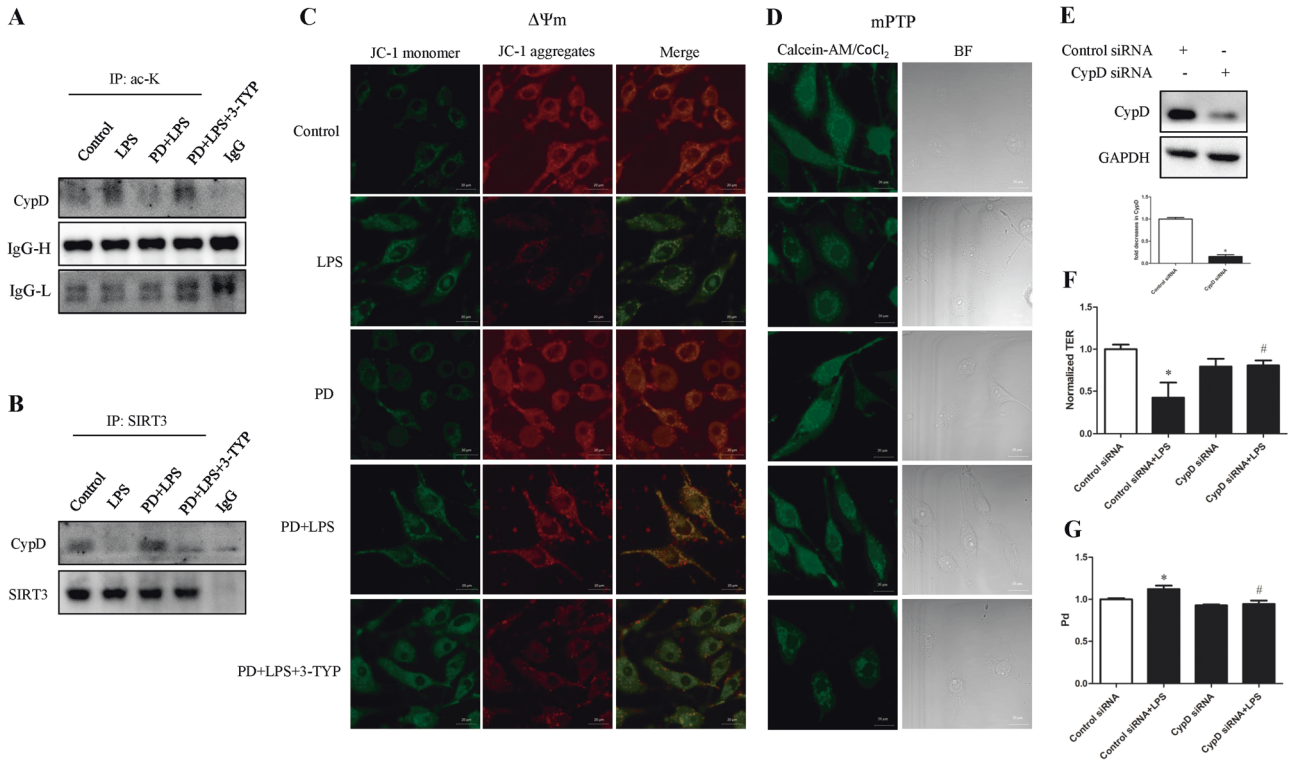

Fig. 8 Effect of SIRT3-mediated CypD deacetylation on PD-mediated endothelial barrier protection. HUVECs were pretreated with PD (50 μM) or PD (50 μM) plus 3-TYP (50 μM) for 2 h, followed by treatment with 1 μg/mL LPS for 12 h. **a**, **b** Whole cell lysates were prepared and probed in co-immunoprecipitation assays with a pan acetyl-lysine antibody (**a**) and an anti-SIRT3 antibody (**b**) respectively. Western blot assays were then performed for the immunoprecipitated samples with an anti-CypD antibody. **c** Mitochondrial membrane potential (ΔΨm) was assessed with JC-1staining: cells in red represent JC-1 aggregates due to an intact ΔΨm. Conversely, cells in green represent JC-1 monomers due to a disrupted ΔΨm. **d** Cells were incubated with calcein-AM and quenching agent $CoCl_2$. The mPTP was monitored by fluorescence of calcein-AM in the mitochondria by confocal and brightfield (BF) microscope. **e** HUVECs were transfected with either control siRNA or CypD siRNA. Protein expression levels of CypD were measured by western blot analysis. **f**–**g** Transfected HUVECs were stimulated with LPS (1 μg/mL) or PBS for 24 h. Endothelial monolayer permeability was assessed by TER (**f**) and flux of FITC-dextran (**g**). $n = 3$. $^{*}P < 0.05$ versus control siRNA, $^{\#}P < 0.05$ versus control siRNA + LPS

maintenance of cadherin–catenin complex and actin cytoskeleton, thus inhibiting LPS-mediated barrier disruption. Whether alteration of TJs is also implicated in the protection of PD remains to be further investigated.

Consistent with our previous findings on septic injury in kidney [8], the deacetylase activity of SIRT3 was downregulated in vascular endothelial cells. In the study of LPS-induced alterations on SIRT3 protein expression, a decreased expression was also observed. Consistently, Zeng et al. previously showed a decreased SIRT3 protein expression in pulmonary endothelial cells after LPS treatment [15]. Intriguingly, the decrease in SIRT3 protein expression occurred later than changes in deacetylase activity. It can be presumed that in the initial stage, LPS mainly influences endothelial permeability by regulating SIRT3 activity, and that in the later stage, SIRT3 protein downregulation is also involved. Therefore, we used SIRT3 specific antagonist as well as overexpression and knockdown strategies to further verify the involvement of SIRT3. Notably, we found that PD provided endothelial barrier protection by, upregulating the activity, as well as the protein expression of SIRT3.

It has been demonstrated that mitochondrial protections such as superoxide clearance and mPTP maintenance can inhibit endothelial hyperpermeability [37, 38]. Previously, we demonstrated that PD mediated mitochondrial protection via activating SIRT3 in small intestine during hemorrhagic shock [9]. In this study, it was established that PD-mediated mitochondrial protection was involved in endothelial barrier protection in a sepsis model. SIRT3-mediated SOD2 deacetylation is one of the most important mitochondrial ROS detoxification mechanisms. In this study, we showed that PD promoted endothelial barrier function through SIRT3-mediated SOD2 deacetylation and activation, and subsequent mitochondrial ROS detoxification.

Moreover, the role of SIRT3-CypD signaling in barrier protection was also identified. SIRT3-mediated deacetylation suppresses CypD activity, and thus inhibits mPTP opening and ΔΨm reduction [16]. In present study, CypD hyperacetylation and decreased interaction with SIRT3

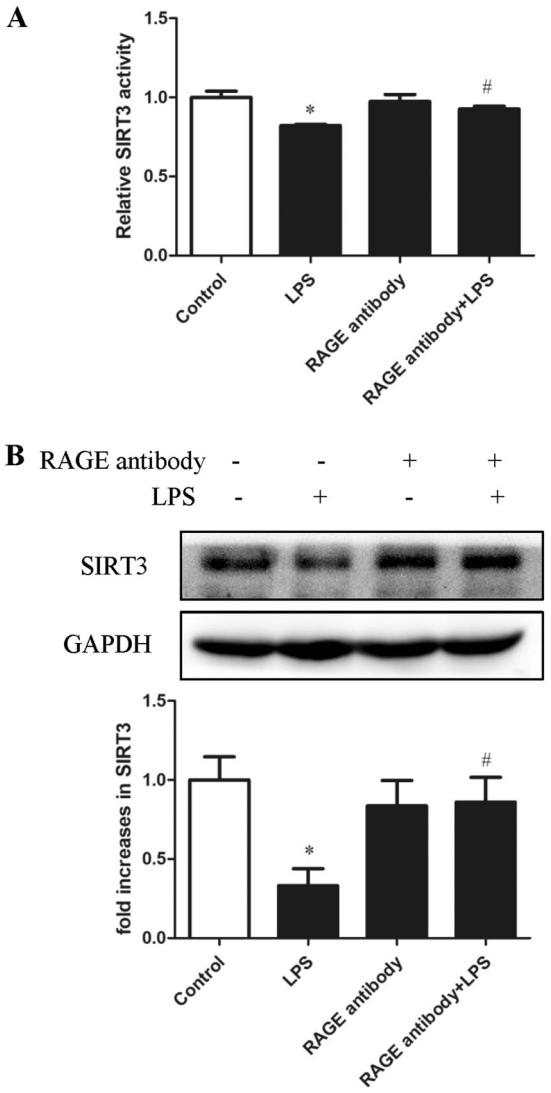

Fig. 9 Involvement of RAGE in LPS-induced alterations of SIRT3 activity and protein expression. HUVECs were pretreated with RAGE blocking antibody (10 μg/mL) or ECM medium for 1 h, followed by stimulation with LPS (1 μg/mL) or PBS for 12 h. **a** SIRT3 activity was determined using a SIRT3 Assay kit. **b** Protein expression levels of SIRT3 were detected by western blot analysis. $n = 3$. $^{*}P < 0.05$ versus control or RAGE antibody, $^{\#}P < 0.05$ versus LPS

were observed in response to LPS challenge, resulting in mPTP opening and subsequent ΔΨm reduction. In a rat model of hemorrhagic shock, inhibition of CypD with cyclosporine A prevented vascular hyperpermeability [38]. CypD-deficient mice also exhibited reduced lung vascular leakage in endotoxemia [39]. It implied that, PD might attenuate the deleterious effects of LPS-induced CypD acetylation via SIRT3 activation. Similarly, our findings showed that CypD knockdown reversed LPS-induced endothelial barrier disruption. Conclusively, it is clear that PD enhances SIRT3-mediated deacetylation of SOD2 and CypD and thus inhibits LPS-induced endothelial barrier disruption by promoting ROS clearance and mPTP maintenance in mitochondria.

Reversible protein acetylation is emerging as an important posttranslational modification involved in various mitochondrial processes. SIRT3-mediated deacetylation of mitochondrial proteins has become a very intense area of research. Here, it was proved that PD activated the "mitochondrial fidelity protein", SIRT3, and hence exerted endothelial barrier protection after LPS treatment by reversible lysine deacetylation of SOD2 and CypD. It could be speculated that, some other mitochondrial targets of SIRT3 may also be implicated in PD-mediated barrier protection.

We previously demonstrated that PD significantly increased the survival rate of septic rats by protecting the mitochondria function of renal tubular epithelial cells (RTECs) [22]. Recently, a study showed that viniferin, a naturally occurring resveratrol dimer, can alleviate LPS-induced acute lung injury by activating SIRT3 and restore macrophage bioenergetic function [40]. Though we used the SIRT3 specific inhibitor in vivo and SIRT3 siRNA in endothelial cells to confirm the protective effects of PD in sepsis, it is possible that some of the beneficial effects of PD may be related to its effects on non-endothelial cells. And other signaling pathways may also participate in PD-mediated barrier protection in sepsis.

In sepsis, Toll-like receptor 4 is the most well-known receptor for LPS. Besides, RAGE was also demonstrated as an important pattern recognition receptor binding directly to LPS. We previously found that LPS upregulated RAGE expression, and that RAGE was involved in LPS-induced endothelial hyperpermeability [20]. Involvement of RAGE in AGE-induced SIRT3 downregulation was evidenced in endothelial progenitor cells (EPCs) [29]. In present study, we showed that RAGE was involved in LPS-induced decrease in SIRT3 deacetylase activity and protein expression. The underlying mechanisms warrant further investigations.

Some limitations of this study cannot be ignored. The human SIRT3 contains two isoforms, a long form (~44 kDa) and a short form (~28 kDa). It has been widely accepted that the short form SIRT3 primarily resides in mitochondria and is more likely to exhibit deacetylase activity [41]. Consequently, in this study, the short form isoform of SIRT3 was observed. However, in a cardiac hypertrophy model, discrepancy of the two SIRT3 isoforms was demonstrated [42]. Further studies need to be done concerning these two isoforms. Moreover, the molecular mechanisms underlying LPS-induced alterations of SIRT3 protein expression is yet to be elucidated. PGC-1α-dependent ERRα-mediated signaling pathway has been demonstrated to regulate SIRT3 protein expression [27]. Further investigations are required to determine whether

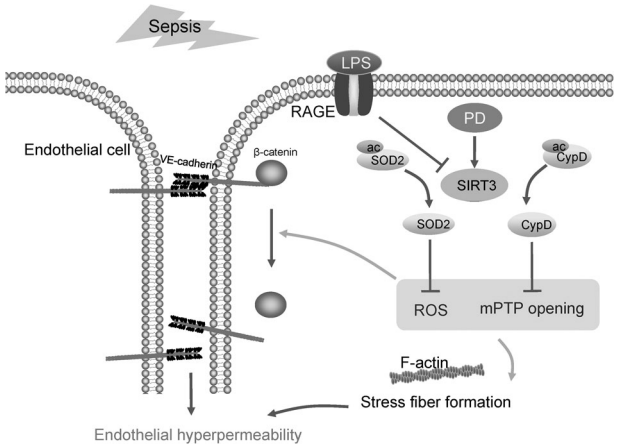

Fig. 10 Schematic illustration of the mechanism underlying the protective role of PD-activated SIRT3 in LPS-induced endothelial barrier disruption. In sepsis, RAGE acts as a negative regulator of SIRT3 via binding with LPS. SIRT3-mediated deacetylation of SOD2 and CypD was inhibited under LPS stimulation, leading to excess mitochondrial ROS formation and mPTP opening. PD promotes SIRT3 activation and protects against endothelial barrier disruption

this signaling pathway participates in LPS-induced SIRT3 alterations.

In conclusion, this study reveals that PD exerts protective effects in LPS-induced endothelial barrier disruption via SIRT3 activation (Fig. 10). During sepsis, SIRT3-mediated deacetylation of mitochondrial SOD2 and CypD is suppressed, leading to mitochondrial dysfunction and subsequent endothelial hyperpermeability. Our findings shed light on potential application of PD as a therapy for sepsis through SIRT3-mediated endothelial barrier protection.

Funding This work was supported by the National Natural Science Foundation of China (81870210, 81170297, 81871604, 81701955, and 81703935), the Guangdong Natural Science Foundation Team Project (S2013030013217), the Natural Science Foundation of Guangdong Province (2016A030313561, 2016A030310389, and 2017A030313590), the Medical Science and Technology Research Fund of Guangdong Province (A2019178), and the Outstanding Youths Development Scheme of Nanfang Hospital, Southern Medical University (2016J011).

Compliance with ethical standards

Conflict of interest The authors declare that they have no conflict of interest.

Publisher's note Springer Nature remains neutral with regard to jurisdictional claims in published maps and institutional affiliations.

References

1. Singer M, Deutschman CS, Seymour CW, Shankar-Hari M, Annane D, Bauer M, et al. The third international consensus definitions for sepsis and septic shock (Sepsis-3). JAMA. 2016;315:801–10.
2. De Backer D, Orbegozo Cortes D, Donadello K, Vincent JL. Pathophysiology of microcirculatory dysfunction and the pathogenesis of septic shock. Virulence. 2014;5:73–9.
3. Geven C, Kox M, Pickkers P. Adrenomedullin and adrenomedullin-targeted therapy as treatment strategies relevant for sepsis. Front Immunol. 2018;9:292.
4. Dejana E, Orsenigo F, Lampugnani MG. The role of adherens junctions and VE-cadherin in the control of vascular permeability. J Cell Sci. 2008;121(Pt 13):2115–22.
5. Mishra R, Singh SK. HIV-1 Tat C phosphorylates VE-cadherin complex and increases human brain microvascular endothelial cell permeability. BMC Neurosci. 2014;15:80.
6. Lee WL, Slutsky AS. Sepsis and endothelial permeability. N Engl J Med. 2010;363:689–91.
7. Zeng Z, Chen Z, Li T, Zhang J, Gao Y, Xu S, et al. Polydatin: a new therapeutic agent against multiorgan dysfunction. J Surg Res. 2015;198:192–9.
8. Xu S, Gao Y, Zhang Q, Wei S, Chen Z, Dai X, et al. SIRT1/3 activation by resveratrol attenuates acute kidney injury in a septic rat model. Oxid Med Cell Longev. 2016;2016:7296092.
9. Zeng Z, Yang Y, Dai X, Xu S, Li T, Zhang Q, et al. Polydatin ameliorates injury to the small intestine induced by hemorrhagic shock via SIRT3 activation-mediated mitochondrial protection. Exp Opin Ther Targets. 2016;20:645–52.
10. Ahn BH, Kim HS, Song S, Lee IH, Liu J, Vassilopoulos A, et al. A role for the mitochondrial deacetylase Sirt3 in regulating energy homeostasis. Proc Natl Acad Sci USA. 2008;105:14447–52.
11. Jing E, O'Neill BT, Rardin MJ, Kleinridders A, Ilkeyeva OR, Ussar S, et al. Sirt3 regulates metabolic flexibility of skeletal muscle through reversible enzymatic deacetylation. Diabetes. 2013;62:3404–17.
12. Samant SA, Zhang HJ, Hong Z, Pillai VB, Sundaresan NR, Wolfgeher D, et al. SIRT3 deacetylates and activates OPA1 to regulate mitochondrial dynamics during stress. Mol Cell Biol. 2014;34:807–19.
13. Sun F, Si Y, Bao H, Xu Y, Pan X, Zeng L, et al. Regulation of sirtuin 3-mediated deacetylation of cyclophilin D attenuated cognitive dysfunction induced by sepsis-associated encephalopathy in mice. Cell Mol Neurobiol. 2017;37:1457–64.
14. Zhao WY, Zhang L, Sui MX, Zhu YH, Zeng L. Protective effects of sirtuin 3 in a murine model of sepsis-induced acute kidney injury. Sci Rep. 2016;6:33201.
15. Zeng H, He X, Tuo QH, Liao DF, Zhang GQ, Chen JX. LPS causes pericyte loss and microvascular dysfunction via disruption of Sirt3/angiopoietins/Tie-2 and HIF-2alpha/Notch3 pathways. Sci Rep. 2016;6:20931.
16. Hafner AV, Dai J, Gomes AP, Xiao CY, Palmeira CM, Rosenzweig A, et al. Regulation of the mPTP by SIRT3-mediated deacetylation of CypD at lysine 166 suppresses age-related cardiac hypertrophy. Aging. 2010;2:914–23.
17. Li P, Meng X, Bian H, Burns N, Zhao KS, Song R. Activation of sirtuin 1/3 improves vascular hyporeactivity in severe hemorrhagic shock by alleviation of mitochondrial damage. Oncotarget. 2015;6:36998–7011.
18. Pi H, Xu S, Reiter RJ, Guo P, Zhang L, Li Y, et al. SIRT3-SOD2-mROS-dependent autophagy in cadmium-induced hepatotoxicity and salvage by melatonin. Autophagy. 2015;11:1037–51.
19. Qiu X, Brown K, Hirschey MD, Verdin E, Chen D. Calorie restriction reduces oxidative stress by SIRT3-mediated SOD2 activation. Cell Metab. 2010;12:662–7.
20. Wang L, Wu J, Guo X, Huang X, Huang Q. RAGE plays a role in LPS-induced NF-kappaB activation and endothelial hyperpermeability. Sensors. 2017;17. PMID: 28358333; https://doi.org/10.3390/s17040722.

21. Tinsley JH, Wu MH, Ma W, Taulman AC, Yuan SY. Activated neutrophils induce hyperpermeability and phosphorylation of adherens junction proteins in coronary venular endothelial cells. J Biol Chem. 1999;274:24930–4.
22. Gao Y, Zeng Z, Li T, Xu S, Wang X, Chen Z, et al. Polydatin inhibits mitochondrial dysfunction in the renal tubular epithelial cells of a rat model of sepsis-induced acute kidney injury. Anesth Analg. 2015;121:1251–60.
23. Chen T, Dai SH, Li X, Luo P, Zhu J, Wang YH, et al. Sirt1-Sirt3 axis regulates human blood–brain barrier permeability in response to ischemia. Redox Biol. 2018;14:229–36.
24. Chen ML, Zhu XH, Ran L, Lang HD, Yi L, Mi MT. Trimethylamine-N-oxide induces vascular inflammation by activating the NLRP3 inflammasome through the SIRT3-SOD2-mtROS signaling pathway. J Am Heart Assoc. 2017;6. PMID: 29118033; https://doi.org/10.1161/JAHA.117.002238.
25. Cheng A, Yang Y, Zhou Y, Maharana C, Lu D, Peng W, et al. Mitochondrial SIRT3 mediates adaptive responses of neurons to exercise and metabolic and excitatory challenges. Cell Metab. 2016;23:128–42.
26. Zeng X, Yang J, Hu O, Huang J, Ran L, Chen M, et al. Dihydromyricetin ameliorates nonalcoholic fatty liver disease by improving mitochondrial respiratory capacity and redox homeostasis through modulation of SIRT3 signaling. Antioxid Redox Signal. 2019;30:163–83.
27. Song C, Zhao J, Fu B, Li D, Mao T, Peng W, et al. Melatonin-mediated upregulation of Sirt3 attenuates sodium fluoride-induced hepatotoxicity by activating the MT1-PI3K/AKT-PGC-1alpha signaling pathway. Free Radic Biol Med. 2017;112:616–30.
28. Parodi-Rullan RM, Chapa-Dubocq X, Rullan PJ, Jang S, Javadov S. High sensitivity of SIRT3 deficient hearts to ischemia-reperfusion is associated with mitochondrial abnormalities. Front Pharmacol. 2017;8:275.
29. Chang M, Zhang B, Tian Y, Hu M, Zhang G, Di Z, et al. AGEs decreased SIRT3 expression and SIRT3 activation protected AGEs-induced EPCs' dysfunction and strengthened anti-oxidant capacity. Inflammation. 2017;40:473–85.
30. Liu TF, Vachharajani V, Millet P, Bharadwaj MS, Molina AJ, McCall CE. Sequential actions of SIRT1-RELB-SIRT3 coordinate nuclear-mitochondrial communication during immunometabolic adaptation to acute inflammation and sepsis. J Biol Chem. 2015;290:396–408.
31. Zheng Z, Ma H, Zhang X, Tu F, Wang X, Ha T, et al. Enhanced glycolytic metabolism contributes to cardiac dysfunction in polymicrobial sepsis. J Infect Dis. 2017;215:1396–406.
32. Pillai VB, Kanwal A, Fang YH, Sharp WW, Samant S, Arbiser J, et al. Honokiol, an activator of Sirtuin-3 (SIRT3) preserves mitochondria and protects the heart from doxorubicin-induced cardiomyopathy in mice. Oncotarget. 2017;8:34082–98.
33. Zhai M, Li B, Duan W, Jing L, Zhang B, Zhang M, et al. Melatonin ameliorates myocardial ischemia reperfusion injury through SIRT3-dependent regulation of oxidative stress and apoptosis. J Pineal Res. 2017;63. PMID: 28500761; https://doi.org/10.1111/jpi.12419
34. Zeng Z, Chen Z, Xu S, Song R, Yang H, Zhao KS. Polydatin alleviates small intestine injury during hemorrhagic shock as a SIRT1 activator. Oxid Med Cell Longev. 2015;2015:965961.
35. Vestweber D, Winderlich M, Cagna G, Nottebaum AF. Cell adhesion dynamics at endothelial junctions: VE-cadherin as a major player. Trends Cell Biol. 2009;19:8–15.
36. Fang D, Hawke D, Zheng Y, Xia Y, Meisenhelder J, Nika H, et al. Phosphorylation of beta-catenin by AKT promotes beta-catenin transcriptional activity. J Biol Chem. 2007;282:11221–9.
37. Dong WW, Liu YJ, Lv Z, Mao YF, Wang YW, Zhu XY, et al. Lung endothelial barrier protection by resveratrol involves inhibition of HMGB1 release and HMGB1-induced mitochondrial oxidative damage via an Nrf2-dependent mechanism. Free Radic Biol Med. 2015;88(Pt B):404–16.
38. Tharakan B, Holder-Haynes JG, Hunter FA, Smythe WR, Childs EW. Cyclosporine A prevents vascular hyperpermeability after hemorrhagic shock by inhibiting apoptotic signaling. J Trauma. 2009;66:1033–9.
39. Fonai F, Priber JK, Jakus PB, Kalman N, Antus C, Pollak E, et al. Lack of cyclophilin D protects against the development of acute lung injury in endotoxemia. Biochim Biophys Acta. 2015;1852:2563–73.
40. Kurundkar D, Kurundkar AR, Bone NB, Becker EJ, Jr., Liu W, Chacko B, et al. SIRT3 diminishes inflammation and mitigates endotoxin-induced acute lung injury. JCI Insight. 2019;4.
41. Schwer B, Bunkenborg J, Verdin RO, Andersen JS, Verdin E. Reversible lysine acetylation controls the activity of the mitochondrial enzyme acetyl-CoA synthetase 2. Proc Natl Acad Sci USA. 2006;103:10224–9.
42. Sundaresan NR, Gupta M, Kim G, Rajamohan SB, Isbatan A, Gupta MP. Sirt3 blocks the cardiac hypertrophic response by augmenting Foxo3a-dependent antioxidant defense mechanisms in mice. J Clin Investig. 2009;119:2758–71.